

Minimal Dark Matter bound states at future colliders

Salvatore Bottaro^a, Alessandro Strumia^b, Natascia Vignaroli^b

^a *Scuola Normale, Pisa, Italia*

^b *Dipartimento di Fisica, Università di Pisa, Italia*

Abstract

The hypothesis that Dark Matter is one electroweak multiplet leads to predictive candidates with multi-TeV masses that can form electroweak bound states. Bound states with the same quantum numbers as electroweak vectors are found to be especially interesting, as they can be produced resonantly with large cross sections at lepton colliders. Such bound states exist e.g. if DM is an automatically stable fermionic weak 5-plet with mass $M \approx 14$ TeV such that the DM abundance is reproduced thermally. In this model, a muon collider could resolve three such bound states. Production rates are so large that details of DM spectroscopy can be probed with larger statistics: we compute the characteristic pattern of single and multiple γ lines.

Contents

1	Introduction	2
2	Minimal Dark Matter and its bound states	3
3	Bound-state production at colliders	5
3.1	Production of $^n s_3$ bound states from $\mu^- \mu^+$ collisions	6
3.2	Production of other bound states from VV collisions	9
3.3	Decays of bound states and their collider signals	10
4	Conclusions	12

1 Introduction

The hypothesis that Dark Matter is the thermal relic of one new multiplet under the Standard Model gauge group provides some predictive allowed candidates [1]. In particular, the cosmological DM abundance is reproduced for TeV-scale values of the DM mass, above the LHC reach. A fermionic 5-plet under $SU(2)_L$ with zero hypercharge is a particularly interesting possibility, being automatically long lived enough to be DM. Its thermal abundance matches the DM density for a mass $M \approx 14$ TeV, after taking into account Sommerfeld and bound-state corrections [2]. Its univocal prediction for direct detection can be tested [1, 3], but its production at colliders would allow to measure more than one number. However, even a giant pp collider at 100 TeV would have a limited reach, up to about 4 TeV [4] (see also [5–8]).

A future muon collider could be built in the existing 27 km LEP/LHC circular tunnel. In such a case, μ^\pm beams can reach the maximal energy \sqrt{s} allowed by magnetic fields. This was $\sqrt{s} \approx 14$ TeV at LHC, but future magnets can realistically increase it up to $\sqrt{s} \sim 30$ TeV. Concerning the integrated luminosity, a value $\mathcal{L} \sim 90/\text{ab}$ at $\sqrt{s} = 30$ TeV is considered possible [9], provided that radiological hazards due to muon decays into neutrinos can be limited.

According to [9], a muon collider with this luminosity cannot probe a Minimal DM 5-plet with $M \approx 14$ TeV, unless experiments are able to find in the beam-related background the tracks left by its charged components, short because produced with non-relativistic velocity (see [10] for possible strategies). Otherwise, missing energy signals tagged by an extra muon or gamma have low cross sections and can only probe 5-plets lighter than about 10 TeV [9].

We show that extra signals arise taking into account that such DM forms weak bound states with binding energy $E_B \sim 100$ GeV. Such bound states annihilate into SM particles (including $\mu^+\mu^-$, for appropriate bound states with the same quantum numbers of electroweak vectors) with a width, $\Gamma_B \sim \alpha_2^5 M$, that is small but not much smaller than the expected energy resolution of a muon collider, $\sigma_E \sim 10^{-3}E$. Production and annihilation of DM bound states B thereby results into a large cross section among visible SM particles,

$$\sigma(\mu^+\mu^- \rightarrow B \rightarrow f\bar{f}) \sim \sigma_{\text{peak}} \frac{\Gamma_B}{\sigma_E} \quad \text{where} \quad \sigma_{\text{peak}} \sim \frac{4\pi}{s} \quad (1)$$

is the maximal cross section allowed by unitarity.

One needs to run around the peak, and the minimal 5-plet DM model allows to predict the DM mass, $M \approx 14$ TeV, from the cosmological DM density. More in general (for example a family of three 5-plets allows for smaller M) one could first discover DM through other signals, measure its mass, and next run on the peak, possibly gradually reducing the beam energy spread σ_E of the collider to achieve the maximal cross section. The energy resolution of a muon collider can be reduced by at least one order of magnitude, down to $\sigma_E \sim 10^{-4}E$, at the price of proportionally reducing its luminosity. We also consider other bound states and pp colliders,

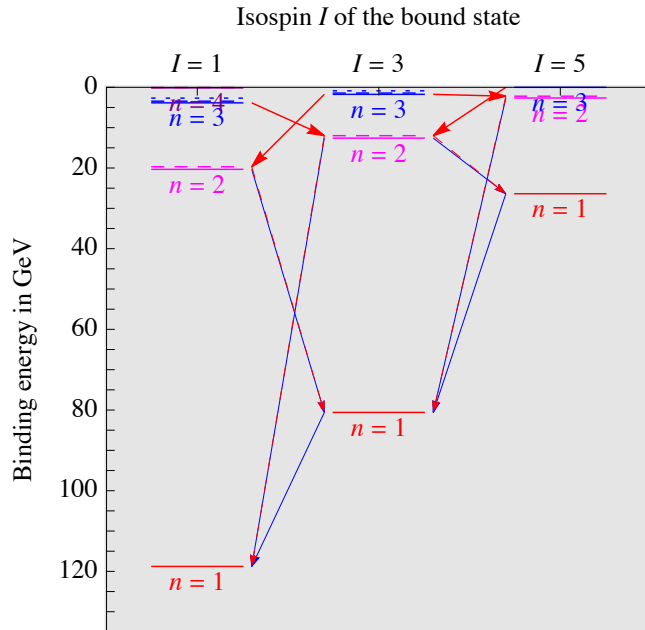


Figure 1: *Energy levels of bound states of two Minimal Dark Matter 5-plets with $M = 14$ TeV. Continuous lines have $\ell = 0$, dashed lines have $\ell = 1$, dotted lines have $\ell = 2$. The blue (red) arrows indicate some main magnetic (electric) decays.*

obtaining small cross sections as no resonant production is possible.¹

The paper is structured as follows. In section 2 we summarize the DM model and the properties of DM bound states. In section 3 we discuss bound state production at colliders, focusing in 3.1 on the main signals from states that can be produced resonantly with large cross section, in 3.2 on other bound states, in 3.3 on rarer but very characteristic signals coming from decays among DM bound states, such as γ lines. In section 4 we give conclusions, and mention one more (curious but small) signal of Minimal DM.

2 Minimal Dark Matter and its bound states

The SM is extended adding a fermionic 5-plet \mathcal{X} under $SU(2)_L$ with zero hypercharge, such that the most general renormalizable Lagrangian is

$$\mathcal{L} = \mathcal{L}_{\text{SM}} + \frac{1}{2} \bar{\mathcal{X}} (i\not{D} + M) \mathcal{X}. \quad (2)$$

¹DM bound states of an electroweak triplet have been discussed in [11] at a pp collider, where no resonant production is possible. We here include important non-abelian Coulomb-like potentials. See also [12].

name ${}^n_J \ell_I^{PC}$	Quantum numbers					Annihilation		Decay	
	n	I	S	ℓ	E_B	Γ_{ann}	into	Γ_{dec}	into
${}^1_1 s_1^{-+}$	1	1	0	0	118 GeV	$3240 \alpha_2^5 M \approx 1.63 \text{ GeV}$	$V\tilde{V}$	0	—
${}^1_1 s_3^{--}$	1	3	1	0	81 GeV	$15625 \alpha_2^5 M/48 \approx 0.17 \text{ GeV}$	$f_L \bar{f}_L + HH^*$	$36 \alpha_2^6 \alpha_{\text{em}} M \approx 4.6 \text{ keV}$	${}^1_{s_1} \gamma$
${}^1_1 s_5^{-+}$	1	5	0	0	26 GeV	$567 \alpha_2^5 M/4 \approx 0.07 \text{ GeV}$	$V\tilde{V}$	$295 \alpha_2^6 \alpha_{\text{em}} M \approx 38 \text{ keV}$	${}^1_{s_3} \gamma$
${}^2_1 s_1^{-+}$	2	1	0	0	20.3 GeV	$405 \alpha_2^5 M \approx 0.2 \text{ GeV}$	$V\tilde{V}$	$13 \alpha_2^6 \alpha_{\text{em}} M \approx 1.7 \text{ keV}$	${}^1_{s_3} \gamma$
${}^2_1 s_3^{--}$	2	3	1	0	13 GeV	$15625 \alpha_2^5 M/384 \approx 21 \text{ MeV}$	$f_L \bar{f}_L + HH^*$	$(6.9 \alpha_2 + 0.3 \alpha_{\text{em}}) \alpha_2^6 M \approx 3.7 \text{ keV}$	${}^1_{s_{1+5}} V$
${}^2_1 s_5^{-+}$	2	5	0	0	2.6 GeV	$567 \alpha_2^5 M/32 \approx 9 \text{ MeV}$	$V\tilde{V}$	$28.4 \alpha_2^6 \alpha_{\text{em}} M \approx 3.6 \text{ keV}$	${}^1_{s_3} \gamma$
${}^2_J p_1^{++}$	2	1	1	1	19.7 GeV	$\mathcal{O}(\alpha_2^7 M) \sim \text{keV}$	VV	$20.4 \alpha_2^4 \alpha_{\text{em}} M \approx 2.5 \text{ MeV}$	${}^1_{s_3} \gamma$
${}^2_J p_3^{+-}$	2	3	0	1	12 GeV	$\mathcal{O}(\alpha_2^8 M) \sim 10 \text{ eV}$	VVV	$(30.2 \alpha_2 + 0.3 \alpha_{\text{em}}) \alpha_2^4 M \approx 15.3 \text{ MeV}$	${}^1_{s_{1+5}} V$
${}^2_J p_5^{++}$	2	5	1	1	2.2 GeV	$\mathcal{O}(\alpha_2^7 M) \sim \text{keV}$	VV	$4.7 \alpha_2^4 \alpha_{\text{em}} M \approx 0.6 \text{ MeV}$	${}^1_{s_3} \gamma$
${}^3_1 s_1^{-+}$	3	1	0	0	3.8 GeV	$120 \alpha_2^5 M \approx 60 \text{ MeV}$	$V\tilde{V}$	$0.34 \alpha_2^4 \alpha_{\text{em}} M \approx 42 \text{ keV}$	${}^2_{p_3} \gamma$
${}^3_1 s_3^{--}$	3	3	1	0	1.7 GeV	$15625 \alpha_2^5 M/1296 \approx 6.0 \text{ MeV}$	$f_L \bar{f}_L + HH^*$	$(0.003 + 0.005) \alpha_2^4 \alpha_{\text{em}} M \approx 1 \text{ keV}$	${}^2_{p_{1+5}} \gamma$
${}^3_1 s_5^{-+}$	3	5	0	0	1.7 MeV	$21 \alpha_2^5 M/4 \approx 2.7 \text{ MeV}$	$V\tilde{V}$	$0.3 \alpha_2^4 \alpha_{\text{em}} M \approx 36 \text{ keV}$	${}^2_{p_3} \gamma$
${}^3_J d_3^{--}$	3	3	1	2	0.9 GeV	$\mathcal{O}(\alpha_2^9 M) \sim \text{eV}$	$f_L \bar{f}_L$	$0.4 \alpha_2^4 \alpha_{\text{em}} M \approx 52 \text{ keV}$	${}^2_{p_{1+5}} \gamma$

Table 1: *Main bound states of fermion weak 5-plets with $M \approx 14 \text{ TeV}$. The parity $P = (-1)^{\ell+1}$ and charge conjugation $C = (-1)^{\ell+S}$ quantum numbers of bound states are broken by chiral weak gauge interactions to SM fermions. Hyper-fine components with different values of J have the same decay rate. Decay rates are not $\text{SU}(2)_L$ -invariant because W, Z emission is sometimes blocked by phase space; we report decay rates averaged over the weak components of bound states.*

The 5-plet contains a Majorana neutral component \mathcal{X}^0 , together with Dirac fermions \mathcal{X}^\pm and $\mathcal{X}^{\pm\pm}$ with charge ± 1 and ± 2 . Due to its electric field, the components with charge q are heavier than \mathcal{X}^0 by $q^2 \Delta M$, where $\Delta M = \alpha_2 M_W \sin^2(\theta_W/2) \approx 166 \text{ MeV}$. Thereby charged states decay into the lightest DM-candidate \mathcal{X}^0 .

The components of \mathcal{X} can be pair-produced at collider. Pairs of 5-plets can form Coulombian-like electroweak bound states given that $M \gtrsim M_{W,Z}/\alpha_2$. Bound states can be computed in components [13], or more simply in $\text{SU}(2)_L$ -symmetric approximation, setting $M_W \approx M_Z$ and neglecting ΔM [2]. States of two quintuplets decompose under $\text{SU}(2)_L$ as $5 \otimes 5 = 1_S \oplus 3_A \oplus 5_S \oplus 7_A \oplus 9_S$. The attractive channels with potential $V = -\alpha_{\text{eff}} e^{-M_{W,Z} r}/r$ have isospin $I = 1$ ($\alpha_{\text{eff}} = 6\alpha_2$), $I = 3$ ($\alpha_{\text{eff}} = 5\alpha_2$), and $I = 5$ ($\alpha_{\text{eff}} = 3\alpha_2$). The SM weak couplings renormalized at TeV energy are $\alpha_2 = 1/30.8$ and $\alpha_{\text{em}} = 1/128.6$. The binding energies of bound states can be approximated as [2]

$$E_B \approx \frac{\alpha_{\text{eff}}^2 M}{4n^2} \left[1 - n^2 y - 0.53 n^2 y^2 \ell(\ell + 1) \right]^2 \quad \text{where} \quad y \approx \frac{1.74 M_{W,Z}}{\alpha_{\text{eff}} M} \quad (3)$$

and ℓ is angular momentum. The bound state exists only when the term in the squared parenthesis is positive. Furthermore, only bound states with $(-1)^{\ell+S+\tilde{I}} = 1$ have the correct fermionic anti-symmetry, where $I = 2\tilde{I} + 1$ is the dimension of the representation. As usual for bound states of two fermions, our states have quantum numbers $C = (-1)^{\ell+S}$ under charge

conjugation and $P = (-1)^{\ell+1}$ under parity (which gets broken when chiral gauge interactions of SM fermions play a role).

The resulting 5-plet bound states at constituent mass $M = 14$ TeV are plotted in fig. 1, and table 1 lists their main properties.² Bound states can decay via annihilation of their constituents with rate Γ_{ann} , or into deeper states with rate Γ_{dec} . Bound states with $J \equiv \ell \oplus S$ equal to 1 or 5 can annihilate into two $SU(2)_L$ vectors VV , while vector bound states with $J = 3$ cannot because of the Landau-Yang theorem.

We are especially interested in bound states that annihilate into SM fermions, as they can thereby be directly produced in $\mu^+\mu^-$ collisions. Such states are those with the same quantum numbers as the weak vectors W_μ^a , so that such bound states mix and inherit couplings to fermions. These special bound states are the ${}^n_1s_3^{--}$ vector triplets with $S = 1$, $\ell = 0$ (the full notation is explained in the first row of table 1), which decay into SM fermions with rate $\Gamma_{\text{ann},f} = 625M/2n^3 = 0.96\Gamma_{\text{ann}}$. The other vector triplet, the ${}^2_1p_3^{+-}$ bound state with $S = 0$, $\ell = 1$, has opposite parity and annihilates in VVV rather than in fermions. The bound state ${}^3_jd_3^{--}$ with $\ell = 2$ has the right quantum numbers, but annihilation rates of bound states with $\ell > 0$ are suppressed by extra powers of α_2 .

Table 1 also shows the decay widths among bound states: their computation will be discussed in section 3.3, where we discuss the associated collider signals.

3 Bound-state production at colliders

All bound states have narrow total width, $\Gamma = \Gamma_{\text{ann}} + \Gamma_{\text{dec}} \ll M$. Then, their collider phenomenology is well approximated *à la* Breit-Wigner such that their decay widths determine their production rates. The cross section for s -channel production is

$$\sigma(i_1i_2 \rightarrow B \rightarrow f) \approx \text{BW}(s)\sigma_{\text{peak}} \quad (4)$$

where

$$\text{BW}(s) = \frac{M_B^2\Gamma_B^2}{(s - M_B^2)^2 + M_B^2\Gamma_B^2} \simeq \Gamma_B M_B \pi \delta(s - M_B^2), \quad \sigma_{\text{peak}} = \frac{16\pi S_B}{M_B^2 S_{i_1} S_{i_2}} \text{BR}_{i_1i_2} \text{BR}_f \quad (5)$$

and S_i is the spin times group multiplicity of the various particles (e.g. 2 for μ^\pm , 3 if B is a vector singlet etc).

The cross section needs to be convoluted with the energy distribution of a muon collider, described by some function $\wp(s)$ normalized as $\int \wp(s)d\sqrt{s} = 1$. Assuming that each beam has

²While we agree with the generic formulæ for the rates in [2], we found a missing order one factor in the application to the 5-plet: the decay rates of the $2p$ states differ from eq. (91) in [2] because a α_2 should be α_{eff} . These $2p$ decay rates negligibly affect the cosmological relic abundance computed in [2].

a Gaussian energy distribution with standard deviation σ_E one gets a Gaussian distribution

$$\wp(s) = \frac{1}{\sqrt{2\pi}\Delta_E} \exp\left[-\frac{(\sqrt{s} - M_B)^2}{2\Delta_E^2}\right], \quad \Delta_E = \sqrt{2}\sigma_E. \quad (6)$$

The energy resolution of a muon collider is expected to be $\sigma_E \approx 10^{-3}E \sim 14 \text{ GeV}$ [14], larger than the widths of bound states, $\Gamma_B \lesssim \text{GeV}$. Thereby a muon collider cannot sit at the peak of the resonances, where the cross section is as large as allowed by unitarity. In the limit $\sigma_E \gg \Gamma_B$ the convoluted cross section is

$$\sigma(i \rightarrow B \rightarrow f) \simeq \epsilon \sigma_{\text{peak}}, \quad \epsilon = \frac{\sqrt{\pi}\Gamma_B}{4\sigma_E}. \quad (7)$$

Thanks to the σ_E at the denominator, bound states that can be directly produced from $i_1 i_2 = \mu^- \mu^+$ collisions can have cross sections comparable or bigger than tree-level SM cross sections, $\sigma \approx 4\pi\alpha_2^2/s$.

3.1 Production of ${}^n s_3$ bound states from $\mu^- \mu^+$ collisions

We here study states that can be directly produced from $\mu^- \mu^+$ collisions with a resonant s -channel cross section. These are the states with the same quantum numbers as electroweak vectors: $I = 3$, $S = 1$ and $PC = --$, achieved in view of the constituent fermion 5-plets \mathcal{X} . The first such state is ${}_{J=1}^{n=1} s_{I=3}^{--}$ (${}^1 s_3$ for short), that exists for $M \gtrsim 4.4 \text{ TeV}$. Table 1 shows that, for $M = 14 \text{ TeV}$, ${}^n s_3$ bound states exist for $n = \{1, 2, 3\}$. The leading-order cross section for s -channel production of their neutral component B^0 is given by eq. (7) with

$$\epsilon \approx \frac{1}{192n^3} \frac{10^{-3}}{\sigma_{E/E}}, \quad \sigma_{\text{peak}}(\mu^+ \mu^- \rightarrow B_{1s_3}^0 \rightarrow f \bar{f}) = \frac{3\pi}{M^2} \text{BR}_\mu \text{BR}_f \approx 30 \text{ fb} \frac{\text{BR}_f}{\text{BR}_\ell} \quad (8)$$

where $\text{BR}_\ell = 1/25$ for any lepton flavour, and $\text{BR}_q = 3/25$ for any quark flavour. The denominator is 25 (rather than 24), taking into account the $1/25$ branching ratio into the Higgs multiplet. A more precise evaluation includes higher order effects. In particular, the signal cross section gets reduced by about a factor 2 taking into account initial state radiation (ISR) of γ and Z . We perform MonteCarlo simulations by approximating such bound states as vectors $B_{n\mu}^a$ coupled as $g_n B_{n\mu}^a (\bar{f} \gamma_\mu T^a f)_L$ to left-handed SM fermions, and choosing couplings g_n that reproduce the bound-state widths. Then, numerical results from MADGRAPH [15] show that γ radiation dominates. Such effect is analytically approximated by assigning a parton distribution function to each muon beam, such that the amount of muons with energy equal to the beam energy gets reduced by an order unity factor, analytically given by $\sim (\Gamma/M)^{4\alpha_{\text{em}} \ln(E/m_\mu)/\pi}$ [17]. Precise analytical results [16] agree with numerical results.

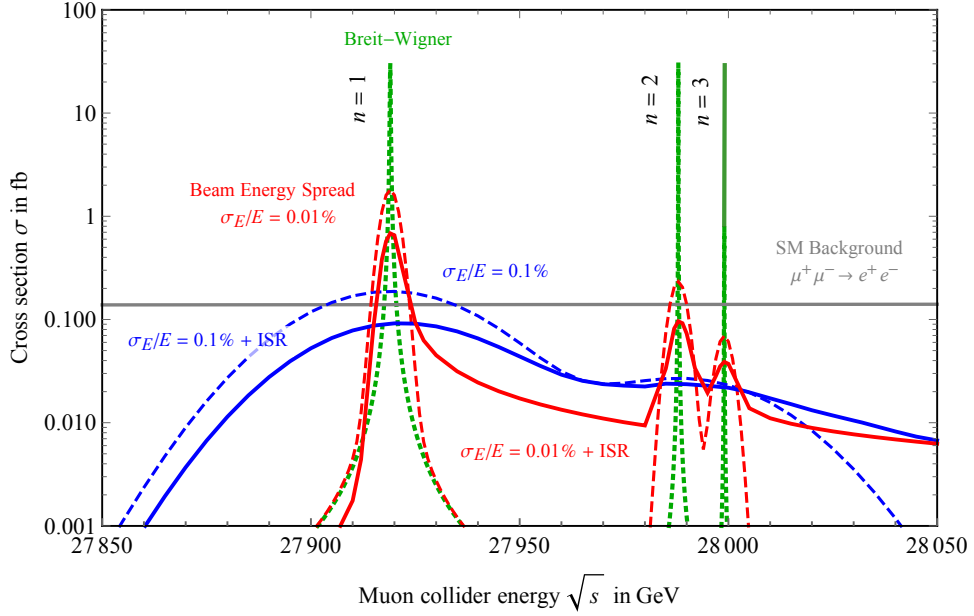


Figure 2: *Bound-state signals of a Minimal Dark Matter 5-plet with constituent mass $M = 14$ TeV. The dotted green curves show the signal cross section for production of ${}^n s_1$ DM bound states with $n = \{1, 2, 3\}$, ignoring the beam energy spread. The dashed curves show the signal cross section, for two different values of the beam energy spread, $\sigma_E = 10^{-3} E$ (baseline value) and $\sigma_E = 10^{-4} E$ (feasible value). The continuous curves show the signal cross section after also taking into account initial state emission. The gray horizontal curve is the SM $\mu^+ \mu^- \rightarrow e^+ e^-$ background.*

Considering, for example, the $e^- e^+$ final state (so that calorimeters can precisely measure their large energy), the SM background is

$$\sigma_{\text{SM}}(\mu^+ \mu^- \rightarrow e^+ e^-) = \frac{4\pi\alpha_{\text{em}}^2}{3s} + \frac{2\pi\alpha_{\text{em}}\alpha_2}{3c_W^2 s}(g_L + g_R)^2 + \frac{\pi\alpha_2^2}{3c_W^4 s}(g_L^2 + g_R^2)^2 \approx 140 \text{ ab} \frac{(28 \text{ TeV})^2}{s} \quad (9)$$

where $s \gg M_Z^2$, $c_W = M_W/M_Z$, $g_L = 1/2 - c_W^2$, $g_R = 1 - c_W^2$. We see that σ_{peak} is 200 times larger than σ_{SM} (green dotted curve in fig. 2) and that a design energy spread reduces it by $\epsilon \sim 1/200$ for $n = 1$, providing a DM signal at the level of total SM backgrounds (dashed blue curve in fig. 2). The $n = 1$ state can be mildly separated from those with $n = \{2, 3\}$, that have rates below the SM background and thereby need some dedicated search.

Fig. 3a shows that the integrated luminosity needed to discover such state corresponds to about one day of running, taking into account its annihilation channels into $e^+ e^-$ and jets and without performing selection cuts (for simplicity, we do not include annihilations into $\mu^+ \mu^-$, which have a larger background due to t -channel vector exchange that can be efficiently reduced

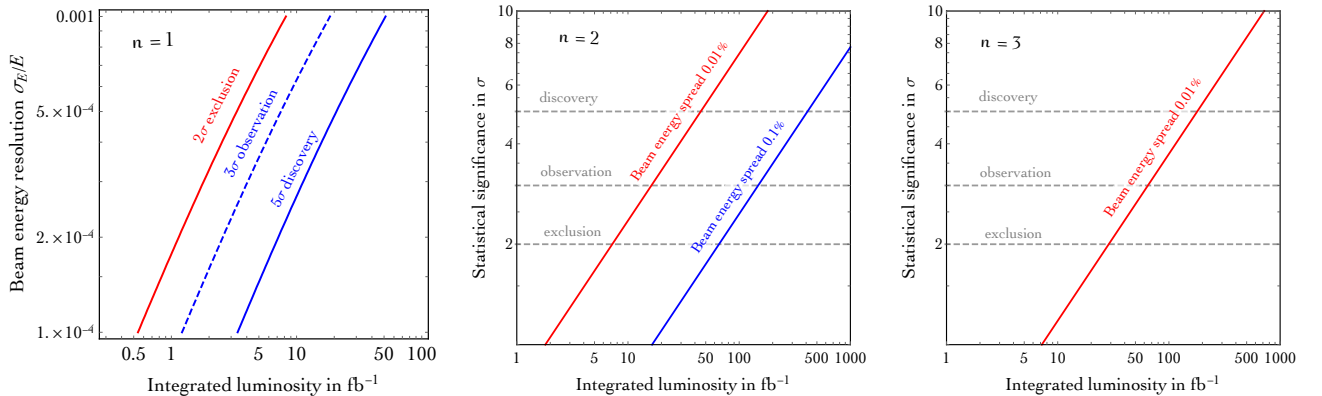


Figure 3: *The integrated luminosity needed to see the $n s_3$ bound states with mass $2M = 28$ TeV of a Minimal DM 5-plet at a muon collider with $s \approx 4M^2$ is much smaller than the possible value, 90/ab at $\sigma_E/E = 10^{-3}$.*

by cuts on p_T and other variables). We assumed a 70% efficiency for detecting each electron or jet in the final state. Reducing the beam energy spread reduces the needed integrated luminosity, but by an amount similar to the expected loss in collider luminosity.

With a feasible reduction of σ_E by one order of magnitude, the cross section for producing the 1s_3 bound state becomes one order of magnitude larger than SM backgrounds, and the excited bound states with $n = 2, 3$ can be separated and acquire total cross sections at the level of the SM backgrounds (dashed red curve in fig. 2). After taking initial state radiation into account, one obtains the continuous curves in fig. 2, where peaks become asymmetric and larger above the threshold due to the ‘radiative return’ phenomenon. Fig. 3b,c show the integrated luminosity needed to discover such states. The non-resonant loop corrections considered by [11] at \sqrt{s} slightly above the $2M$ threshold interfere destructively with the SM background leading to a decrease of the SM cross section by up to 8%.

The charged components B_μ^\pm of the isospin triplet of bound states are produced with a relatively large cross section, given that the partonic neutrino component of a μ^\pm beam is peaked at energy fraction $x = 1$ [18], in view of soft W^\pm emission. By running a bit above the peak, the state with $n = 1$ is produced as $\mu^+\mu^- \rightarrow B_\mu^\pm W_\mu^\mp$ with fb-scale cross section, as shown by the blue curve in fig. 4.

Finally, we mention that the state 3d_3 too has the same quantum numbers as electroweak vectors and can thereby be produced directly from $\mu^+\mu^-$ collision; however its annihilation rate (see bottom row of table 1) is highly suppressed by $\alpha_2^{5+2\ell}$ in view of $\ell = 2$ and we neglect it.

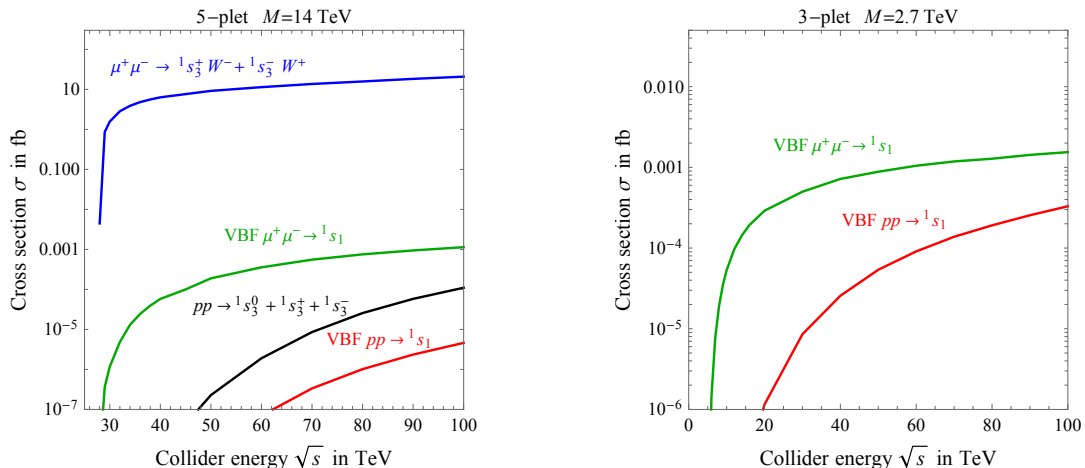


Figure 4: Cross sections for the production of some bound states of the Minimal DM fermionic 5-plet with constituent mass $M = 14$ TeV (left) and of the fermionic 3-plet with $M = 2.7$ TeV (right) at a $\mu^+\mu^-$ collider and at a pp collider.

3.2 Production of other bound states from VV collisions

The other bound states annihilate to weak vectors and can thereby be produced through associated production via vectors. Then, the energy spread in the effective collision energy becomes large, $\sigma_E \sim \sqrt{s}$, and the cross sections small. These more general processes can be computed using automated codes [15], approximating bound states as particles with effective couplings to their decay products that reproduce the widths [19] computed in table 1. For example, the ground pseudo-scalar bound state 1s_1 with $I = 1$ can be written as a scalar singlet B coupled as $B\epsilon_{\mu\nu\mu'\nu'}V_{\mu\nu}^aV_{\mu'\nu'}^a$. The pseudo-scalar bound state 1s_5 with $I = 5$ can be written as a scalar $B_{aa'}$ in the symmetric trace-less representation of $SU(2)_L$ coupled as $B_{aa'}\epsilon_{\mu\nu\mu'\nu'}V_{\mu\nu}^aV_{\mu'\nu'}^{a'}$.

We focus on the ground state 1s_1 , as it has the largest annihilation rate. It can be produced via scatterings of SM electroweak vectors, $\gamma\gamma \rightarrow B_{1s_1}$, $\gamma\mu^\pm \rightarrow B_{1s_1}\mu^\pm$, $\mu^+\mu^- \rightarrow B_{1s_1}\mu^+\mu^-$, $\mu^+\mu^- \rightarrow B_{1s_1}\nu_\mu\bar{\nu}_\mu$. Resonant production is not possible and one thereby must run at higher $\sqrt{s} > 2M$: the green curve in fig. 4 shows that, as expected, the production cross section is much smaller.

The red curve in fig. 4 shows its analogous production cross sections at a pp collider, which is even smaller given that vector partons in a p beam have lower energy than in a μ beam. For completeness, the black curve in fig. 4 shows the cross section for production at a pp collider of the 1s_3 bound state discussed in the previous section. We do not discuss the backgrounds.

Furthermore, we consider a Wino-like Minimal DM fermionic triplet. The DM abundance

is reproduced thermally for $M = 2.7 \text{ TeV}$. At this mass only one 1s_1 bound state exists with $E_B \approx 68 \text{ MeV}$ and $\Gamma_B = 8\alpha_2^5 M \approx 4 \text{ MeV}$ [2]. This bound state cannot be produced with a resonantly-enhanced cross section. Fig. 4b shows its production cross section at a muon or pp collider.

3.3 Decays of bound states and their collider signals

In this section we describe the computation of the bound state decays listed in table 1, having in mind that we seek characteristic collider signals produced by decays among bound states. The leading-order decays $B \rightarrow B'V$ proceed through the emission of a weak vector boson V , which is often a photon as the phase space for W, Z emission is often closed. Such process dominantly occurs via electric dipole transitions, although magnetic dipole transitions happen to be important in cases where selection rules forbid electric dipole transitions. We compute bound states in the $SU(2)_L$ -symmetric approximation, so that bound states of two 5-plets have two indices ij in the 5 representation, that can be converted into isospin eigenstates $B_{\tilde{I}\tilde{I}_3}$ through Clebsch-Gordan coefficients: $B_{ij} = C_{ij}^{\tilde{I}\tilde{I}_3} B_{\tilde{I}\tilde{I}_3}$.

- The effective interaction hamiltonian for the electric dipole at leading order is

$$H_{\text{el}} = -\frac{g_2}{M} [\vec{A}^a(x_1) \cdot \vec{p}_1 T_{i'i}^a \delta_{jj'} + \vec{A}^a(x_2) \cdot \vec{p}_2 \bar{T}_{j'j}^a \delta_{ii'}] + g_2 \alpha_2 [\vec{A}^a(0) \cdot \hat{r}] T_{i'i}^b \bar{T}_{j'j}^c f^{abc} \quad (10)$$

leading to the following selection rules: $|\Delta\tilde{I}| = 1$, $|\Delta\ell| = 1$, $\Delta S = 0$. Decay rates are obtained as

$$\Gamma(^2p_{\tilde{I}} \rightarrow ^1s_{\tilde{I}'} + V^a) = \frac{16}{9I_{2p}} \frac{\alpha_2 k}{M^2} \sum_{\tilde{I}_3 \tilde{I}'_3} \left| \int r^2 dr R_{\tilde{I},2p} \left(C_{\mathcal{J}}^{a\tilde{I}_3 \tilde{I}'_3} \partial_r - C_{\mathcal{T}}^{a\tilde{I}_3 \tilde{I}'_3} \frac{\alpha_2 M}{2} \right) R_{\tilde{I}',1s} \right|^2 \quad (11)$$

$$\Gamma(^3s_{\tilde{I}} \rightarrow ^2p_{\tilde{I}'} + V^a) = \frac{16}{3I_{3s}} \frac{\alpha_2 k}{M^2} \sum_{\tilde{I}_3 \tilde{I}'_3} \left| \int r^2 dr R_{\tilde{I}',2p} \left(C_{\mathcal{J}}^{a\tilde{I}_3 \tilde{I}'_3} \partial_r + C_{\mathcal{T}}^{a\tilde{I}_3 \tilde{I}'_3} \frac{\alpha_2 M}{2} \right) R_{\tilde{I},3s} \right|^2 \quad (12)$$

where r is the radius, $R(r)$ are normalized radial wave-functions, k is the spatial momentum of V , I is the isospin of the initial bound state, and

$$C_{\mathcal{J}}^{a\tilde{I}_3 \tilde{I}'_3} = \frac{1}{2} \text{Tr} \left[C^{\tilde{I}' \tilde{I}'_3} \left\{ C^{\tilde{I} \tilde{I}_3}, T^a \right\} \right], \quad C_{\mathcal{T}}^{a\tilde{I}_3 \tilde{I}'_3} = i \text{Tr} \left[C^{\tilde{I}' \tilde{I}'_3} T^b C^{\tilde{I} \tilde{I}_3} T^c \right] f^{abc}. \quad (13)$$

- The effective interaction hamiltonian for the magnetic dipole at leading order is (see e.g. [20])

$$H_{\text{mag}} = -\frac{g_2}{2M} [T_{i'i}^a \delta_{jj'} \vec{\sigma} \cdot \vec{B}^a(x_1) + \bar{T}_{j'j}^a \delta_{ii'} \vec{\sigma} \cdot \vec{B}^a(x_2)] + \dots \quad (14)$$

leading to the following selection rules: $|\Delta\tilde{I}| = 1$, $\Delta\ell = 0$, $|\Delta S| = 1$. Decay rates are obtained as [20]

$$\Gamma(^{n_i} s_{\tilde{I}_i} \rightarrow ^{n_f} s_{\tilde{I}_f} + V^a) = \frac{2^3}{I_i} \frac{\alpha_2 k^3}{M^2} \sum_{\tilde{I}_3, i \tilde{I}_3, f} \left| C_{\mathcal{J}}^{a\tilde{I}_3, i \tilde{I}_3, f} \int r^2 dr R_{n_i s_{\tilde{I}_i}} R_{n_f s_{\tilde{I}_f}} \right|^2 \quad (15)$$

with no contribution from the omitted non-abelian term in eq. (14).

- Higher-order interactions lead to multiple-vector emission, with suppressed rates that turn out to be negligible.

As discussed in section 3.1, the lightest bound state that can be produced resonantly is the neutral component of 1s_3 . This is the only component of 1s_3 that can decay (W^\pm emission from charged components of 1s_3 is kinematically blocked) to $^1s_1\gamma$ via a magnetic transition with a rate $\Gamma_{\text{dec}} = 3 \times 4.6 \text{ keV}$. Such rate is of order $\alpha_2^6 \alpha_{\text{em}} M$, where an α_2^2 factor arises from the γ phase space; another α_2^4 from the magnetic field \vec{B}^a ; the α_{em} from photon emission. Taking into account its annihilation rate, the neutral component of the 1s_3 bound state decays into a monochromatic γ with energy $E_\gamma \approx 38 \text{ GeV}$ with branching ratio $\text{BR}_{\text{dec}} \approx 9 \cdot 10^{-5}$. This corresponds to 19 events in a run with baseline $\sigma_E = 10^{-3}$ and luminosity $\mathcal{L} = 90/\text{ab}$.

Higher order states are produced with a lower cross section, that scales as $\Gamma_{\text{ann}} \propto 1/n^3$. Nevertheless, such states could give a higher rate of decay events, proportional to $\sigma \text{BR}_{\text{dec}} \propto \Gamma_{\text{ann}} \times \Gamma_{\text{dec}}/\Gamma_{\text{ann}} \propto \Gamma_{\text{dec}}$.

- At $n = 2$, the 2s_3 bound state similarly decays magnetically, with the difference that it can now also emit massive weak bosons, and decay into multiple states $^1s_1, ^1s_5$ (we neglect decays in 2s_1 because their rate is negligibly small, at eV level). The neutral component of 2s_3 decays emitting a γ with rate $\Gamma_{\text{dec}} \approx 2.0 \text{ keV}$ and emitting a Z with rate $\Gamma_{\text{dec}} \approx 1.7 \text{ keV}$; charged components have similar decay rates. In view of the lower binding energy and wave-function overlap, 2s_3 thereby gives a similar number of decay events as 1s_3 . As a result, the γ decays of the 2s_3 neutral component produces two distinctive single-photon lines, at $E_\gamma \approx 105 \text{ GeV}$ and 13 GeV , as well as Z bosons.
- At $n = 3$, the 3s_3 bound state can decay electrically into $^2p_{1+5}\gamma$, with a rate of order $\alpha_2^4 \alpha_{\text{em}} M$ (where an α_2^2 factors arises from the γ phase space; another α_2^2 from the dipole matrix element; the α_{em} from photon emission). The numerical coefficient turns however to be small, and the decay rate is again around a keV. More precisely, only the neutral component can decay into 2p_1 , and all components decay equally into 2p_5 . Thereby, table 1 implies that the decay rate of the neutral component is $\Gamma_{\text{dec}} = (3 \times 0.003 + 0.005) \alpha_2^4 \alpha_{\text{em}} \approx 1.7 \text{ keV}$. The $^2p_{1+5}$ bound states next dominantly decay via a large electric dipole into 1s_3 , that annihilates. This process thereby gives a set of multiple-photon lines, with $E_\gamma \approx \{18 \text{ GeV}, 60 \text{ GeV}\}$, and with $E_\gamma \approx \{0.5 \text{ GeV}, 79 \text{ GeV}\}$. As signal events have very distinctive $\gamma\gamma$ signatures, backgrounds can be strongly reduced.

For completeness, in table 1 we also computed decay rates of other states that cannot be produced resonantly with large rates. Thereby we do not discuss them. All above numbers assume $M = 14 \text{ TeV}$ and need to be recomputed otherwise.

4 Conclusions

We considered DM as electroweak multiplets, and studied the effects of their electroweak bound states at future colliders. We found that bound states with the same quantum numbers as electroweak vectors can be produced resonantly with large cross sections by running lepton colliders at the appropriate \sqrt{s} . Such bound states exist if DM is a heavy enough fermionic multiplet.³ A wino-like weak fermionic triplet with ‘thermal’ mass that reproduces the cosmological DM density, $M = 2.7 \text{ TeV}$, does not form such bound states. Three of such bound states arise if DM is an automatically-stable fermionic weak 5-plet with ‘thermal’ mass $M \approx 14 \text{ TeV}$. The level structure is plotted in fig. 1, the main properties of the bound states are computed in table 1, and fig. 2 shows that the three predicted peaks would be easily observable at a muon collider, running at $\sqrt{s} \approx 2M$ and with a beam energy spread $\sigma_E/E = 10^{-3}$ or better. The production rates of the neutral components B_n^0 of the bound-state triplets are so large that one day of running may be enough for discovery, see fig. 3. One could next search for rarer but more characteristic sets of single and multiple lines γ produced by decays among bound states, as discussed in section 3.3. The charged components B_n^\pm of the bound state triplets can also be produced with partially enhanced cross section at a broader $\sqrt{s} \gtrsim 2M$, as neutrinos have a peaked partonic distribution in muons.

We also studied the other bound states that cannot be produced resonantly. The extra 5-plet bound states in table 1, as well as the only bound state formed by a 3-plet, are produced at $\mu^+\mu^-$ or pp colliders with small non-resonant cross sections as shown in fig. 4.

As an aside final comment, we mention a new Minimal DM signal even more futuristic than a muon collider.⁴ DM \mathcal{X}^0 gravitationally attracted by a neutron star reaches relativistic velocity before hitting its surface, so that charged current scatterings such as $\mathcal{X}^0 n \rightarrow \mathcal{X}^- p$ and $\mathcal{X}^0 p \rightarrow \mathcal{X}^+ n$ become kinematically allowed despite the $\Delta M \approx 166 \text{ MeV}$ gap, and have a large tree-level cross section $\sigma \sim m_n^2/v^4 \sim 10^{-38} \text{ cm}^2$. Decays of charged components can then produce neutrinos with energy around 10 MeV at rate $\dot{N}_\nu \sim \dot{M}/\Delta M \sim 10^{25}/\text{sec}$. Here $\dot{M}_{\text{DM}} = \rho_{\text{DM}} v_{\text{DM}} \pi b^2$ is the DM mass that falls in the neutron star. The impact parameter is $b/R_{\text{ns}} = v_{\text{esc}}/v_{\text{DM}}/\sqrt{1-v_{\text{esc}}^2}$ where $R_{\text{ns}} \sim (M_{\text{Pl}}/m_n)^3 \sim \text{few km}$ is the radius of the neutron star, and $v_{\text{esc}} \sim 1$ is the escape velocity. Given that the nearest neutron stars are expected to be at distance $d \sim \text{pc}$ from the Earth, the resulting neutrino flux $\Phi_\nu \sim \dot{N}_\nu/4\pi d^2$ is about 10 orders of magnitude below the expected background of supernova neutrinos. A very futuristic detector close to a neutron star is needed to reveal the signal.

³A similar resonant enhancement arises from bound states with the same quantum numbers as the Higgs boson, possibly present in speculative DM models where the Higgs mediates attractive forces between DM constituents, fermionic or bosonic.

⁴A.S. thanks Paolo Panci and Raghuv eer Garani for pointing it out.

Acknowledgements We thank Michele Redi, Andrea Wulzer and Ivano Basile. This work was supported by the ERC grant 669668 NEO-NAT and by PRIN 2017FMJFMW.

References

- [1] M. Cirelli, N. Fornengo, A. Strumia, “[Minimal dark matter](#)”, Nucl.Phys.B 753 (2006) 178 [[arXiv:hep-ph/0512090](#)].
- [2] A. Mitridate, M. Redi, J. Smirnov, A. Strumia, “[Cosmological Implications of Dark Matter Bound States](#)”, JCAP 05 (2017) 006 [[arXiv:1702.01141](#)].
- [3] J. Hisano, K. Ishiwata, N. Nagata, “[QCD Effects on Direct Detection of Wino Dark Matter](#)”, JHEP 06 (2015) 097 [[arXiv:1504.00915](#)].
- [4] Contribution by B. Ostdiek, “[Physics at a 100 TeV \$pp\$ collider: beyond the Standard Model phenomena](#)” [[arXiv:1606.00947](#)].
- [5] M. Cirelli, F. Sala, M. Taoso, “[Wino-like Minimal Dark Matter and future colliders](#)”, JHEP 10 (2014) 033 [[arXiv:1407.7058](#)].
- [6] B. Ostdiek, “[Constraining the minimal dark matter fiveplet with LHC searches](#)”, Phys.Rev.D 92 (2015) 055008 [[arXiv:1506.03445](#)].
- [7] T. Han, S. Mukhopadhyay, X. Wang, “[Electroweak Dark Matter at Future Hadron Colliders](#)”, Phys.Rev.D 98 (2018) 035026 [[arXiv:1805.00015](#)].
- [8] M. Saito, R. Sawada, K. Terashi, S. Asai, “[Discovery reach for wino and higgsino dark matter with a disappearing track signature at a 100 TeV \$pp\$ collider](#)”, Eur.Phys.J.C 79 (2019) 469 [[arXiv:1901.02987](#)].
- [9] T. Han, Z. Liu, L.-T. Wang, X. Wang, “[WIMPs at High Energy Muon Colliders](#)” [[arXiv:2009.11287](#)].
- [10] R. Capdevilla, F. Meloni, R. Simoniello, J. Zurita, “[Hunting wino and higgsino dark matter at the muon collider with disappearing tracks](#)” [[arXiv:2102.11292](#)].
- [11] T. Katayose, S. Matsumoto, S. Shirai, “[Non-perturbative Effects on Electroweakly Interacting Massive Particles at Hadron Collider](#)” [[arXiv:2011.14784](#)].
- [12] W. Shepherd, T.M.P. Tait, G. Zaharijas, “[Bound states of weakly interacting dark matter](#)”, Phys.Rev.D 79 (2009) 055022 [[arXiv:0901.2125](#)]. H. An, B. Echenard, M. Pospelov, Y. Zhang, “[Probing the Dark Sector with Dark Matter Bound States](#)”, Phys.Rev.Lett. 116 (2016) 151801 [[arXiv:1510.05020](#)]. Y. Tsai, L.-T. Wang, Y. Zhao, “[Dark Matter Annihilation Decay at The LHC](#)”, Phys.Rev.D 93 (2016) 035024 [[arXiv:1511.07433](#)]. A. Kroyi, I. Low, Y. Zhang, “[Broadening Dark Matter Searches at the LHC: Mono-X versus Darkonium Channels](#)”, JHEP 10 (2018) 026 [[arXiv:1807.07972](#)]. L. Di Luzio, R. Gröber, G. Panico, “[Probing new electroweak states via precision measurements at the LHC and future colliders](#)”, JHEP 01 (2019) 011 [[arXiv:1810.10993](#)]. Y. Tsai, T. Xu, H.-B. Yu, “[Displaced Lepton Jet Signatures from Self-Interacting Dark Matter Bound States](#)”, JHEP 08 (2019) 131 [[arXiv:1811.05999](#)].
- [13] M. Cirelli, A. Strumia, M. Tamburini, “[Cosmology and Astrophysics of Minimal Dark Matter](#)”, Nucl.Phys.B 787 (2007) 152 [[arXiv:0706.4071](#)].
- [14] J.P. Delahaye, M. Diemoz, K. Long, B. Mansoulié, N. Pastrone, L. Rivkin, D. Schulte, A. Skrinsky, A. Wulzer, “[Muon Colliders](#)” [[arXiv:1901.06150](#)].
- [15] J. Alwall, R. Frederix, S. Frixione, V. Hirschi, F. Maltoni, O. Mattelaer, H.-S. Shao, T. Stelzer, P. Torrielli, M. Zaro, “[The automated computation of tree-level and next-to-leading order](#)

- differential cross sections, and their matching to parton shower simulations”, JHEP 07 (2014) 079 [arXiv:1405.0301].
- [16] S. Jadach, B.F.L. Ward, Z. Was, “Coherent exclusive exponentiation for precision Monte Carlo calculations”, Phys.Rev.D 63 (2001) 113009 [arXiv:hep-ph/0006359].
- [17] M. Greco, T. Han, Z. Liu, “ISR effects for resonant Higgs production at future lepton colliders”, Phys.Lett.B 763 (2016) 409 [arXiv:1607.03210].
- [18] T. Han, Y. Ma, K. Xie, “High energy leptonic collisions and electroweak parton distribution functions”, Phys.Rev.D 103 (2021) L031301 [arXiv:2007.14300].
- [19] Y. Kats, M.D. Schwartz, “Annihilation decays of bound states at the LHC”, JHEP 04 (2010) 016 [arXiv:0912.0526].
- [20] R. Mahbubani, M. Redi, A. Tesi, “Dark Nucleosynthesis: Cross-sections and Astrophysical Signals”, JCAP 02 (2021) 039 [arXiv:2007.07231].